nature geoscience

LETTERS

PUBLISHED ONLINE: 28 FEBRUARY 2010 | DOI: 10.1038/NGEO776

Landslide erosion controlled by hillslope material

Isaac J. Larsen[1]*, David R. Montgomery[1] and Oliver Korup[2†]

Steep hillslopes in mountain belts are eroded by landslides, and landsliding is ultimately driven by the topographic relief produced by fluvial and glacial erosion[1–5]. Landslide erosion rates are derived from estimates of landslide volume and can help to appraise landscape responses to tectonic, climatic and anthropogenic forcing. However, the scaling relationships—power-law equations that are used to estimate the volume of the landslide from the area of the failure—are derived from a limited number of measurements, and do not discriminate between bedrock and soil landslides. Here we use a compilation of landslide geometry measurements from 4,231 individual landslides to assess the relative volume–area scaling of bedrock and soil landslides. We find that shallow, soil-based landslides can be approximated by an exponent of $\gamma = 1.1$–1.3. In contrast, landslides that involve the failure of bedrock have a deeper scar area, and hence larger volume, and are characterized by $\gamma = 1.3$–1.6. On the basis of observations that soil residence times in uplifting mountains can be as low as a few centuries[6], we suggest that both deep bedrock and frequent, shallow soil landslides can erode steep hillslopes at rates commensurate with even rapid tectonic uplift.

Quantifying rates of landslide erosion is essential for understanding links between physical erosion, chemical weathering and atmospheric CO_2 consumption[7,8], the transport of organic carbon from the terrestrial biosphere to ocean basin sinks[9,10], coupling among tectonic, atmospheric and surface processes[11], the productivity and sustainability of soil resources[12] and the forecasting of landslide hazards[13]. However, landslide erosion and the associated transport of soil, rock and biogeochemical constituents are difficult to quantify, in part because regional inventories contain hundreds to thousands of landslides, making it impractical to measure the depth of each landslide scar for determination of eroded volume. Hence, landslide volume and erosion estimates rely on scaling relationships based on relatively few field measurements[2,14–16], where the predicted volume V of a given landslide area A depends on a scaling exponent γ and intercept α such that $V = \alpha A^{\gamma}$. Such a model was first proposed over four decades ago[17]. Among the many subsequent studies of landslide scaling, limited data from New Zealand[2] were used to propose that landslide scar depth scales with landslide width. The resulting self-similar scaling with $\gamma = 1.5$ has been widely used outside New Zealand to estimate landslide volumes and erosion rates[7,13–15,18–21]. Recently, scaling with $\gamma = 1.45$ was proposed on the basis of 677 landslide measurements[22], leading to conclusions that V–A scaling is not significantly influenced by the geomorphic or mechanical properties of the failed soil or bedrock and that γ may vary with landslide size. Although these results draw on several landslide studies emphasizing V–A scaling, V is generally calculated as the product of A and mean landslide depth D, which introduces strong V–A covariance. Moreover, the tacit generality of these γ-values remains untested, or inferred from sample sizes constituting small fractions of published landslide inventories[22].

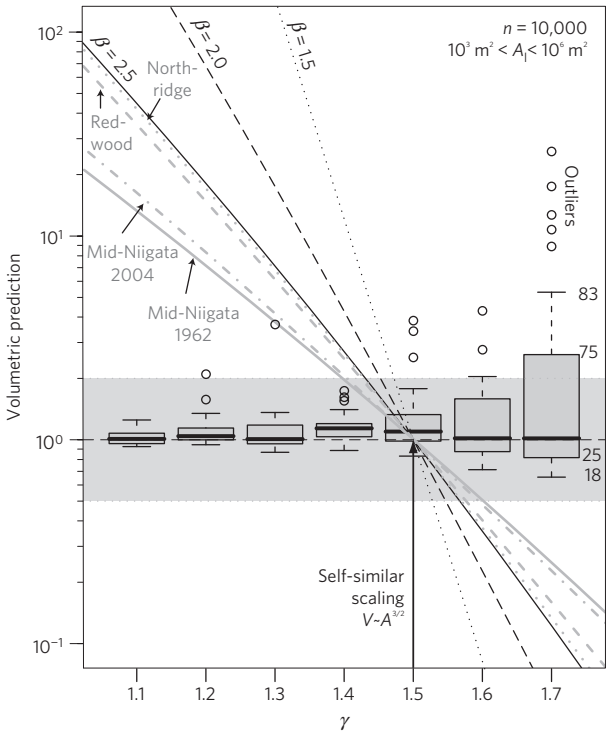

Figure 1 | Effect of the volume–area scaling exponent γ on predicted total landslide volume (V_T). The total volumetric prediction is expressed as the ratio $V_{T(\gamma=1.5)}/V_{T(\gamma)}$ for three synthetic power-law distributed inventories (black lines) and four empirical landslide inventories (grey lines) of landslide area A. The grey shaded area encompasses factor of two under-/over-estimates. The boxes and whiskers show ranges of volumetric prediction for 30 randomly generated inventories of A for a fixed γ. Volumetric estimates from any two inventories with the same size range and scaling parameters generally vary by less than a factor of two, with the variance of the error increasing with γ, which is generally smaller than errors introduced by even small differences in γ. See Supplementary Methods for data sources.

We assessed the degree to which variance in γ affects landslide erosion predictions with a sensitivity analysis that estimates the maximum degree of under- or over-prediction of total landslide volume (V_T), from a given inventory of landslide areas. The analysis shows that small differences in γ lead to substantial variance in V_T predictions. For example, using $\gamma = 1.5$ instead of $\gamma = 1.4$ overestimates V_T by at least a factor of two (Fig. 1). Prediction errors become larger with increasing difference in γ, decreasing area–frequency scaling exponents and increasing

[1]Department of Earth and Space Sciences and Quaternary Research Center, University of Washington, Seattle, Washington 98195-1310, USA, [2]Swiss Federal Research Institutes WSL/SLF, Flüelastr. 11, CH-7260 Davos, Switzerland. †Present address: Institut für Erd- und Umweltwissenschaften, Universität Potsdam, D-14476 Potsdam, Germany. *e-mail: larseni@uw.edu.

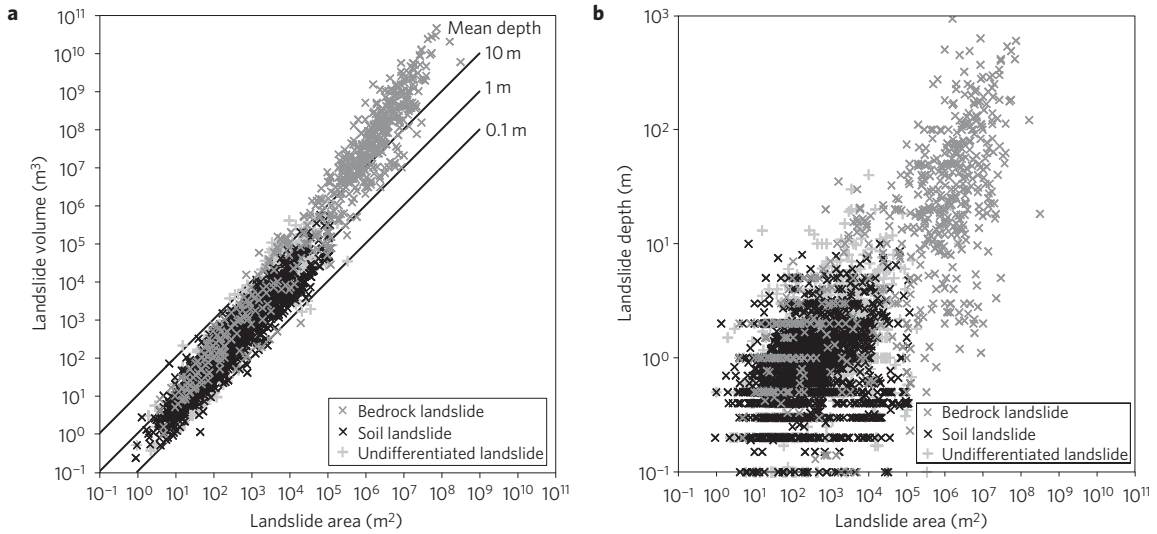

Figure 2 | Landslide geometry scaling. Landslide volume versus area (**a**) and depth versus area (**b**). Data are for bedrock landslides ($n = 604$), soil landslides ($n = 2{,}136$) and undifferentiated landslides ($n = 1{,}491$). The landslide volume–area data may be described by power-law scaling with log $\alpha = -0.836 \pm 0.015$ with units $[L^{(3-2\gamma)}]$, $\gamma = 1.332 \pm 0.005$ and $R^2 = 0.95$. Depth–area data may be described by log $\alpha = -1.090 \pm 0.015$ with units $[L^{(1-2\gamma)}]$, $\gamma = 0.420 \pm 0.005$ and $R^2 = 0.50$. The soil landslide data include 1,617 and 124 measurements of scar and deposit geometry, respectively. The bedrock landslide data include 168 and 344 measurements of scar and deposit geometry, respectively.

maximum landslide area, and can easily be one or more orders of magnitude. The degree of potential over- and under-estimation of landslide erosion is therefore large enough to warrant caution when applying any scaling relationship outside the region it was developed. Inappropriate use of self-similar scaling can lead to substantial errors in landslide volume predictions, and it follows that accurate estimation of γ may have a hitherto unrecognized role in quantifying landslide erosion and mass fluxes.

The lack of accurate constraints on γ for different hillslope materials is a key limitation for quantifying material transfer from uplands to lowlands, particularly as little is known about the relative contributions of soil (which we consider here as unconsolidated soil, regolith and colluvium) and bedrock landslides in denuding mountains. This is a major shortcoming, as on one hand it has been proposed that bedrock landsliding is the only hillslope process capable of keeping pace with the rapid, 1–10 mm yr^{-1} long-term rates of river incision and exhumation of mid- to upper-crustal rocks inferred from studies of uplifting mountains[23]. This rate control may be manifest in adjusted frequencies or magnitudes of landslides on threshold hillslopes (those as steep as can be supported by their material strength). On the other hand, landslide erosion in soil-mantled landscapes may be limited by the rate at which bedrock weathers and is converted to soil[24]. Conceptual landscape evolution models hold that a transition from soil to bedrock landsliding in tectonically active mountains occurs where rock uplift rates greatly exceed soil formation rates[23]. If landslides dominate hillslope erosion through stripping of the soil mantle, soil depths should limit landslide scar depths. We tested the hypothesis that differing limits to bedrock and soil landslide depths are mirrored in distinctly different V–A scaling parameters by compiling and analysing 4,231 measurements of scar and deposit geometry for landslides from around the world, constituting to our best knowledge the largest database of this kind (Supplementary Table S1). We demonstrate that scaling parameters vary significantly with material type, propose a physical basis for this variance and assess whether erosion by soil landslides is capable of keeping pace with bedrock uplift in tectonically active mountain ranges.

The documented landslides show power-law scaling over nine orders of magnitude in A and twelve orders of magnitude in V, with $\gamma = 1.332 \pm 0.005\,(\pm 1\sigma)$ (Fig. 2a). The high scatter in D–A data indicates considerable heterogeneity in measured landslide geometries (Fig. 2b). We examine the heterogeneity in landslide geometry by focusing on V–A scaling exponents because γ facilitates comparison with previous studies. Scaling exponents for bedrock and soil landslides differ significantly, with $\gamma_{\mathrm{rock}} = 1.35 \pm 0.01$ and $\gamma_{\mathrm{soil}} = 1.145 \pm 0.008$, which indicates V–A scaling varies with hillslope material. The combined data set consisting of all soil failures shows that scar depth or deposit thickness does not vary with landslide area, whereas the median depths of soil landslide scars increase by less than one order of magnitude with increasing landslide area (Fig. 3). In contrast, bedrock failures tend to become deeper and their deposits thicken by 2–3 orders of magnitude as landslide areas increase. This trend holds for the combined data set consisting of all bedrock failures, as well as data specifically from measurements of scars or deposits. The depths of small bedrock landslides ($<10^3$ m^2) are similar to soil landslides, probably because they occur in weathered or closely jointed bedrock mechanically similar to soil. Scaling exponents for global bedrock landslides derived from measurements of deposit ($\gamma = 1.40 \pm 0.02$) versus scar ($\gamma = 1.41 \pm 0.02$) geometry are indistinguishable (Supplementary Table S1). Hence, the tendency for detached landslide masses to increase in volume because of dilation and entrainment[25] has not introduced significant errors in our scaling relationships (Supplementary Fig. S1).

Stratifying landslide data by region and dominant material confirms the trend in the combined, global data set and shows that for bedrock landslides γ_{rock} ranges from 1.3 to 1.6, whereas for soil landslides $\gamma_{\mathrm{soil}} = 1.1$–$1.4$ (Fig. 4). Self-similar scaling captures the central tendency in empirical γ-values for data sets consisting primarily of large bedrock landslides, but the large error bars do not allow us to resolve how generally self-similar scaling applies. The systematically lower γ-values show that self-similar scaling does not characterize soil landslides. We argue that the variation in γ for soil landslides reflects regional differences in soil thickness that limit landslide scar depths. For example, the lowest γ-values are from landscapes in British Columbia subject to Pleistocene glaciation and the semi-arid Transverse Ranges of southern California where soils tend to be thinner than in temperate-humid climates.

Systematic offsets in the peaks of estimated probability densities for global soil landslide and soil depths (Fig. 5a) support the notion

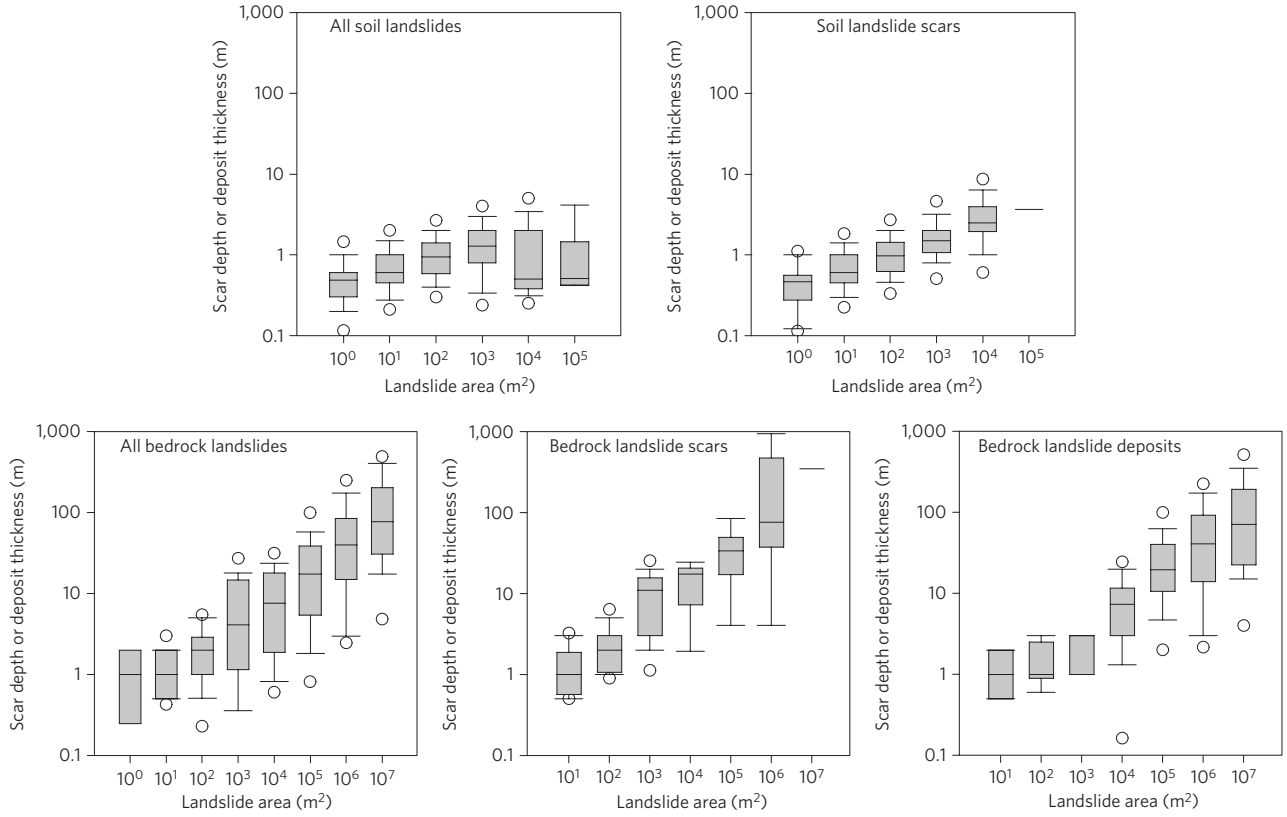

Figure 3 | Box plots of landslide scar depth and deposit thickness as a function of landslide area for soil and bedrock landslides. Landslide areas are binned at one order of magnitude intervals. The horizontal line defines the median, for $n \geq 3$ the box defines the inter-quartile range, and for $n \geq 9$ the whiskers delineate the 10th and 90th percentiles and the circles delineate the 5th and 95th percentiles.

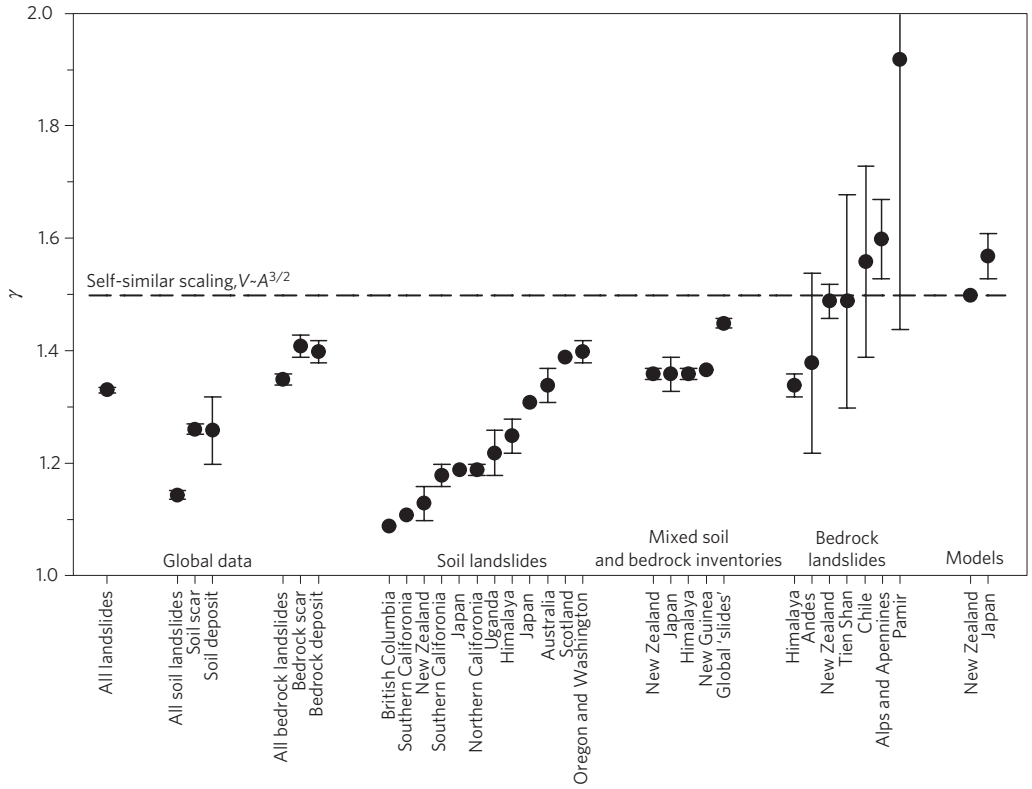

Figure 4 | Scaling exponents (γ) from the landslide data sets used in this study, previous empirical studies and previous models. Landslide inventories are classified on the basis of the dominant landslide type. The circles are mean or reported values and the error bars denote one standard error or reported errors. The data sources are listed in Supplementary Table S1 and the associated intercept (α) values are shown in Supplementary Fig. S2.

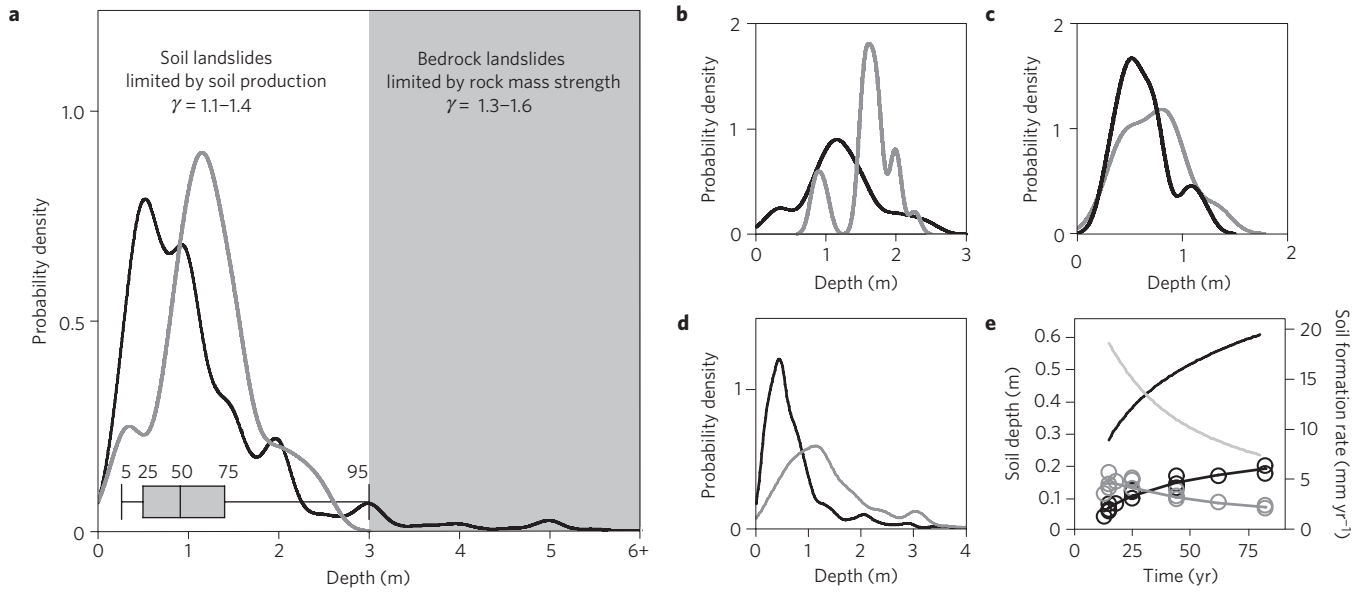

Figure 5 | Soil and landslide depths. a–d, Gaussian kernel density estimates of landslide scar and soil depths for global soil landslides ($n = 1,617$; truncated at 6 m) and global soils ($n = 83$) for slope angles >20° (**a**), Redwood Creek, California (**b**), San Gabriel Mountains, California (**c**) and Oregon Coast Range (**d**). The black (grey) lines show landslide scar (soil) depth. The box plot shows the percentage of landslide depths that are less than the indicated value. The maximum soil depth in the global database and the 95th percentile soil landslide depth are both ~3 m. **e**, Soil depth (black) and rate of soil formation (grey) versus time since landsliding for landslide scars in Tairawhita[27] (upper curves) and Taranaki[28], New Zealand (lower curves).

that scar depths of shallow, primarily soil landslides are limited by soil thickness, and explain systematic differences between soil and bedrock landslide scaling. Regional data from the western US show consistently that modal landslide scar depths are several decimetres less than modal soil depths (Fig. 5b–d). The limiting factor of soil thickness indicates soil landslides on soil-mantled hillslopes characterized by $\gamma < 1.3$ are transport-limited in the short-term if detaching less than the maximum soil depth, but supply-limited in the long-term as soil formation rates dictate the availability of detachable material[26]. If soil formation rates fail to match erosion rates, then bedrock failures with $\gamma > 1.4$ will characterize hillslope erosion, independent of soil cover or formation. The depth distributions for soil and bedrock landslide scars thus provide a physical explanation for variations in γ and we argue that γ is a metric capable of differentiating between these first-order material controls on hillslope erosion, thereby delimiting a transition that is central to understanding the production, transport and loss of soil and the resulting biogeochemical fluxes from mountain landscapes.

The view that only bedrock landslides can match river incision and exhumation rates in rapidly uplifting mountains[23] is supported by observations that bedrock-landslide inventories are dominated volumetrically by fewer, but larger failures more than are inventories of mixed or shallow landslides[20]. However, soil production rates decline exponentially as soil depth increases[24], so conversely, soil production should commensurately accelerate after landsliding removes the soil. Consequently, episodic soil landslides that reduce soil depths will increase rates of bedrock weathering in proportion to their frequency[7]. More frequent landslides will result in enhanced weathering[7] and we propose that bioturbation caused by root penetration into weathered and tectonically fractured bedrock drives rapid soil production in humid mountain belts. Indeed, soil residence times in rapidly uplifting, but soil-mantled landscapes can be as low as 100–200 yr (ref. 6). Rates of soil formation on landslide scars can increase to many times the long-term landscape erosion rates, reaching rates of 5–20 mm yr^{-1} in the century following failure[27,28] (Fig. 5e). Although some soil in landslide scars may derive from upslope soil erosion[27,28], such colluvial material helps accelerate soil production by providing substrate for rapid vegetation re-establishment[29]. Our data set lacks temporal information needed to assess volume–frequency relations for soil versus bedrock landslides, but recent modelling suggests smaller landslides (which tend to be soil failures) may occur frequently enough to contribute equally to denudation as larger failures[21]. We propose that rapid bedrock weathering and soil formation following soil landsliding may allow adjustments in landslide frequency to offset rock uplift without widespread, deep-seated bedrock failures by occurring at commensurately higher frequencies to counterbalance their lower volumetric contributions for a given failure area.

Quantification of the controls on landslide volume–area scaling highlights the importance of discriminating between soil and bedrock landslides when estimating erosion rates. Our analysis shows that soil depth limits the volume of material eroded from soil landslides and that the potential for rapid soil formation could allow soil landsliding to keep pace with rock uplift, even in the most tectonically active mountain ranges. The potential for both soil and bedrock landsliding to keep pace with rock uplift has important implications for soil residence times, biogeochemical cycling and landscape evolution in mountain belts.

Methods

Sensitivity analysis. We created synthetic power-law distributed landslide inventories ($n = 10,000$ each) over a pre-defined range of non-cumulative area–frequency scaling exponents ($\beta = 1.5$, 2.0 and 2.5) and landslide areas (10^3 m$^2 < A_l < 10^6$ m^2), thus encompassing most published inventories. We used different values of γ (with intercept = 0.02 m$^{3-2\gamma}$) and computed the ratio of V_T for $\gamma = 1.5$ over V_T for a range of reported values of γ to determine how variation in γ affects total landslide volume for the synthetic landslide inventories. The range of $V_{T(\gamma=1.5)}/V_{T(\gamma)}$ ratios shown by the boxes and whiskers is for 30 randomly generated inventories of A (all with $\beta = 2.5$; $n = 10,000$ and 10^3 m$^2 < A < 10^6$ m^2) for a fixed γ. See Supplementary Methods for information on empirical inventories. Note that the Northridge landslide inventory has $\beta = 2.4$ only over a limited area range, hence the slightly higher apparent value of β.

Landslide geometry. Measurements of the area, thickness and volume of landslide scars and deposits were obtained from publications, digitized from published figures and our own field measurements (see Supplementary Table S1 for data sources). Data are based on individual measurements and not on extrapolation. Landslide is defined broadly to include rotational, translational, flow and avalanche failures in earth, debris and bedrock[30]. We calculated landslide volume as the product of scar

area and mean scar depth or deposit area and mean deposit thickness, depending on the available data. However, for some data sets landslide area was not defined or was based on the total area disturbed. All data were used to determine the relationship shown in Fig. 2. We further distinguished: (1) bedrock failures, (2) 'soil' failures within unconsolidated soil, regolith or colluvium and (3) undifferentiated failures (Supplementary Fig. S3), as well as data based on: (1) the failure scar geometry, (2) the deposit geometry and (3) other or undefined geometries (Supplementary Fig. S4). Reduced major axis regression on log-transformed data was used to determine the scaling parameters γ and α for different study regions grouped by dominant landslide material (Supplementary Figs S5–S7). Scaling exponents were considered to be significantly different if the 95% confidence intervals did not overlap.

Soil depths. The distribution of global soil landslide scar depths ($n = 1{,}617$) was compared against 83 global upland soil depth values from slopes >20° using Gaussian kernel density estimation. Landslide ($n = 898$) and soil depth ($n = 23$) distributions were also compared for Redwood Creek, California, where landslide and soil depth data were available for the same watershed, and for the San Dimas Experimental Forest, California ($n = 29$) and the Oregon Coast Range ($n = 287$), where landslide and soil depths were measured at individual failures (see Supplementary Information for data sources). Soil depths for Redwood Creek were based on soil pits on slopes >20°. The pits did not always reach unweathered bedrock and thus, in some cases, soil depths are minimum values.

Received 30 October 2009; accepted 18 January 2010; published online 28 February 2010

References

1. Burbank, D. *et al.* Bedrock incision, rock uplift and threshold hillslopes in the northwestern Himalayas. *Nature* **379,** 505–510 (1996).
2. Hovius, N., Stark, C. & Allen, P. Sediment flux from a mountain belt derived by landslide mapping. *Geology* **25,** 231–234 (1997).
3. Schmidt, K. & Montgomery, D. Limits to relief. *Science* **270,** 617–620 (1995).
4. Whipple, K., Kirby, E. & Brocklehurst, S. Geomorphic limits to climate-induced increases in topographic relief. *Nature* **401,** 39–43 (1999).
5. Korup, O. *et al.* Giant landslides, topography, and erosion. *Earth. Planet. Sci. Lett.* **261,** 578–589 (2007).
6. Basher, L., Tonkin, P. & McSaveney, M. Geomorphic history of a rapidly uplifting area on a compressional plate boundary: Cropp River, New Zealand. *Z. Geomorphol.* **69,** 117–131 (1988).
7. Gabet, E. A theoretical model coupling chemical weathering and physical erosion in landslide-dominated landscapes. *Earth. Planet. Sci. Lett.* **264,** 259–265 (2007).
8. Raymo, M. & Ruddiman, W. Tectonic forcing of late Cenozoic climate. *Nature* **359,** 117–122 (1992).
9. Hilton, R. *et al.* Tropical-cyclone-driven erosion of the terrestrial biosphere from mountains. *Nature Geosci.* **1,** 759–762 (2008).
10. Hilton, R., Galy, A. & Hovius, N. Riverine particulate organic carbon from an active mountain belt: Importance of landslides. *Glob. Biogeochem. Cycles* **22,** GB1017 (2008).
11. Willett, S. D., Hovius, N., Brandon, M. T. & Fisher, D. M. *Tectonics, Climate, and Landscape Evolution* (Geol. Soc. Am., 2006).
12. Blaschke, P., Trustrum, N. & Hicks, D. Impacts of mass movement erosion on land productivity: A review. *Prog. Phys. Geog.* **24,** 21–52 (2000).
13. Malamud, B., Turcotte, D., Guzzetti, F. & Reichenbach, P. Landslide inventories and their statistical properties. *Earth Surf. Processes Landforms* **29,** 687–711 (2004).
14. Hovius, N., Stark, C., Hao-Tsu, C. & Jiun-Chuan, L. Supply and removal of sediment in a landslide-dominated mountain belt: Central Range, Taiwan. *J. Geol.* **108,** 73–89 (2000).
15. Lavé, J. & Burbank, D. Denudation processes and rates in the Transverse Ranges, southern California: Erosional response of a transitional landscape to external and anthropogenic forcing. *J. Geophys. Res.* **109,** F01006 (2004).
16. Imaizumi, F. & Sidle, R. Linkage of sediment supply and transport processes in Miyagawa Dam catchment, Japan. *J. Geophys. Res.* **112,** F03012 (2007).
17. Simonett, D. in *Landform studies from Australia and New Guinea* (eds Jennings, J. N. & Mabbutt, J. A.) 64–84 (Australian National Univ. Press, 1967).
18. Niemi, N., Oskin, M., Burbank, D., Heimsath, A. & Gabet, E. Effects of bedrock landslides on cosmogenically determined erosion rates. *Earth. Planet. Sci. Lett.* **237,** 480–498 (2005).
19. Yanites, B., Tucker, G. & Anderson, R. Numerical and analytical models of cosmogenic radionuclide dynamics in landslide-dominated drainage basins. *J. Geophys. Res.* **114,** F01007 (2009).
20. Dussauge, C., Grasso, J. & Helmstetter, A. Statistical analysis of rockfall volume distributions: Implications for rockfall dynamics. *J. Geophys. Res.* **108,** 2286 (2003).
21. Stark, C. & Guzzetti, F. Landslide rupture and the probability distribution of mobilized debris volumes. *J. Geophys. Res.* **114,** F00A02 (2009).
22. Guzzetti, F., Ardizzone, F., Cardinali, M., Rossi, M. & Valigi, D. Landslide volumes and landslide mobilization rates in Umbria, central Italy. *Earth Planet. Sci. Lett.* **279,** 222–229 (2009).
23. Burbank, D. Rates of erosion and their implications for exhumation. *Mineral. Mag.* **66,** 25–52 (2002).
24. Heimsath, A., Dietrich, W., Nishiizumi, K. & Finkel, R. The soil production function and landscape equilibrium. *Nature* **388,** 358–361 (1997).
25. Hungr, O. & Evans, S. Entrainment of debris in rock avalanches: An analysis of a long run-out mechanism. *Geol. Soc. Am. Bull.* **116,** 1240–1252 (2004).
26. Carson, M. & Kirkby, M. *Hillslope Form and Process* (Cambridge Univ. Press, 1972).
27. Smale, M., McLeod, M. & Smale, P. Vegetation and soil recovery on shallow landslide scars in Tertiary hill country, East Cape Region, New Zealand. *New Zeal. J. Ecol.* **21,** 31–41 (1997).
28. Trustrum, N. A. & De Rose, R. C. Soil depth-age relationship of landslides on deforested hillslopes, Taranaki, New Zealand. *Geomorphology* **1,** 143–160 (1988).
29. Restrepo, C. *et al.* Landsliding and its multiscale influence on mountainscapes. *Bioscience* **59,** 685–698 (2009).
30. Cruden, D. & Varnes, D. in *Landslides Investigation and Mitigation. Special Report 247* (eds Turner, A. K. & Schuster, R. L.) 36–71 (Transportation Research Board, National Research Council, National Academy Press, 1996).

Acknowledgements

We thank M. Allen, P. Flentje, J. Griffiths, R. Guthrie, F. Imaizumi, J. Iwahashi, H. Kelsey, A. Knappen, M. A. Madej, Y. Martin, C. May, L. Owen, C. Pain, L. Reid, A. Strom, J. Poesen, R. Sidle, M. Van Den Eeckhaut and H. Yamagishi for generously sharing landslide data and A. Heimsath for a stimulating discussion. I.J.L. thanks Sigma Xi and the Washington NASA Space Grant Consortium for support.

Author contributions

All authors contributed to data compilation, analysis and writing. I.J.L. primarily conducted the data compilation and analysis.

Additional information

The authors declare no competing financial interests. Supplementary information accompanies this paper on www.nature.com/naturegeoscience. Reprints and permissions information is available online at http://npg.nature.com/reprintsandpermissions. Correspondence and requests for materials should be addressed to I.J.L.